Results from the test bench of the Geometry Monitoring System of the ALICE Muon Spectrometer

R. Tieulent, A. Béteille, J.-Y. Grossiord, V. Kakoyan, S. Kox, M. Méziane, J.F. Muraz, Philippe Pillot

EUROPEAN ORGANIZATION FOR NUCLEAR RESEARCH
European Laboratory for Particle Physics

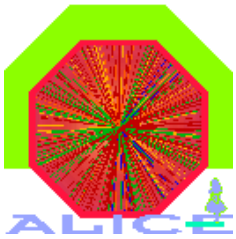

Internal Note/Muon Arm
ALICE reference number
ALICE-INT-2007-010 version 1.0

Date of last change
28.02.2007

Results from the test bench of the Geometry Monitoring System of the ALICE Muon Spectrometer

Authors:

R. Tieulent [a,1], A. Béteille [b], J.-Y. Grossiord [a], V. Kakoyan [c], S. Kox [b], M. Méziane [b], J.-F. Muraz [b] and P. Pillot [a,b]

[a]IPN-Lyon, IN2P3-CNRS et Université Claude Bernard, Lyon-I, France
[b]LPSC-Grenoble, IN2P3-CNRS et Université Joseph Fourier, Grenoble-I, France
[c]Yerevan Physics Institute, Br. Alikhanian st. 2, 375036 Yerevan, Armenia

We present the results obtained with the test bench of the Geometry Monitoring System (GMS) for the ALICE Muon Spectrometer. It consists in a mock up, reproducing at full scale, three half planes of the chambers 6, 7 and 8 of the spectrometer.
We show that the GMS is able to measure transverse displacements with an accuracy of 1.5 μm. We show also that the resolution deteriorates by a factor 3 to 4 when thermal gradients are generated.

Results from the test bench of the Geometry Monitoring System of the ALICE Muon Spectrometer

R. Tieulent [a,1], A. Béteille [b], J.-Y. Grossiord [a], V. Kakoyan [c], S. Kox [b], M. Méziane [b], J.-F. Muraz [b] and P. Pillot [a,b]

[a] *IPN-Lyon, IN2P3-CNRS et Université Claude Bernard, Lyon-I, France*

[b] *LPSC-Grenoble, IN2P3-CNRS et Université Joseph Fourier, Grenoble-I, France*

[c] *Yerevan Physics Institute, Br. Alikhanian st. 2, 375036 Yerevan, Armenia*

Abstract

We present the results obtained with the test bench of the Geometry Monitoring System (GMS) for the ALICE Muon Spectrometer. It consists in a mock up, reproducing at full scale, three half planes of the chambers 6, 7 and 8 of the spectrometer. We show that the GMS is able to measure transverse displacements with an accuracy of 1.5 μm. We show also that the resolution deteriorates by a factor 3 to 4 when thermal gradients are generated.

1 Introduction

ALICE is the only experiment dedicated to the study of nucleus-nucleus collisions at the LHC. Its aim is the physics of strongly interacting matter at extreme energy densities, where is expected the formation of a new phase of matter, the quark-gluon plasma (QGP). One of the most promising probes of the QGP is the production of heavy quarkonium states (J/Ψ, Ψ', Υ, Υ', Υ'') which will be detected via their muonic decays in a forward muon spectrometer[1,2]. Its tracking system consists of ten planes of cathod pad chambers and has to measure the invariant mass of the dimuon system with a resolution, $\Delta M_{\mu^+\mu^-}/M_{\mu^+\mu^-}$, of about 1%. In particular, in order to separate the different particles of the upsilon family ($M_{\mu^+\mu^-} \sim 10$ GeV/c^2), it is necessary to have a mass resolution of about 100 MeV/c^2. This requirement determines the spatial resolution of the muon tracking chambers, which is about 100 microns. This implies that the positions of all tracking chambers have to be monitored with a resolution better than 40 μm [3]. The Geometry Monitoring System (GMS) is the device dedicated to this office.

[1] Contact Person: tieulent@in2p3.fr

The GMS is made of an array of about 460 optical sensors which are installed on platforms located at each corner of the tracking chambers. Two different types of optical devices were adopted: the BCAM and the so-called Proximity. In both devices the image of an object is projected on a CCD sensor through a lens. Then the analysis of the captured image provides a displacement measurement. The most relevant difference between the two systems is represented by the luminous object used. For the BCAM, which is a long-range system, the object is a pair of point-like LEDs, while it is a coded mask for the Proximity which is used for small distances. Figure 1 shows an example of images taken with a BCAM (left) and a Proximity (right). A complete description of the system can be found in [3].

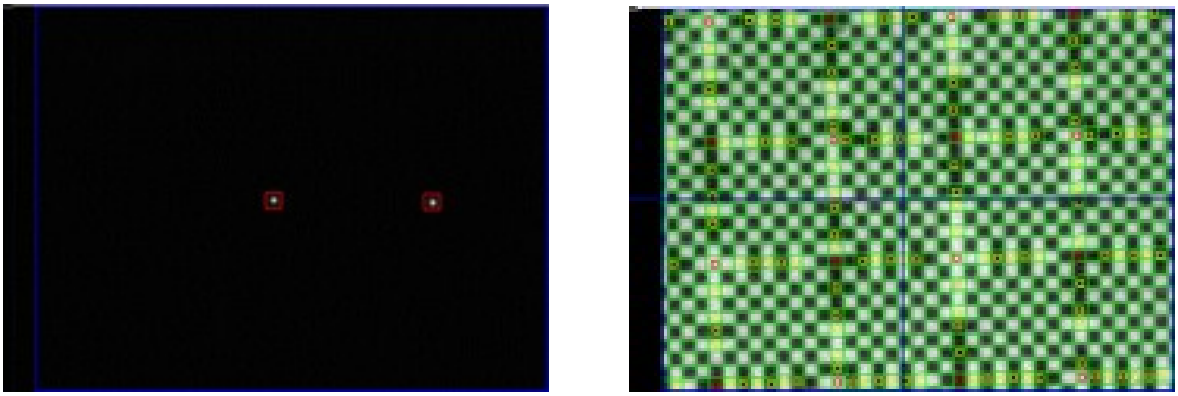

Figure 1: Images taken with a BCAM (left) and a Proximity (right).

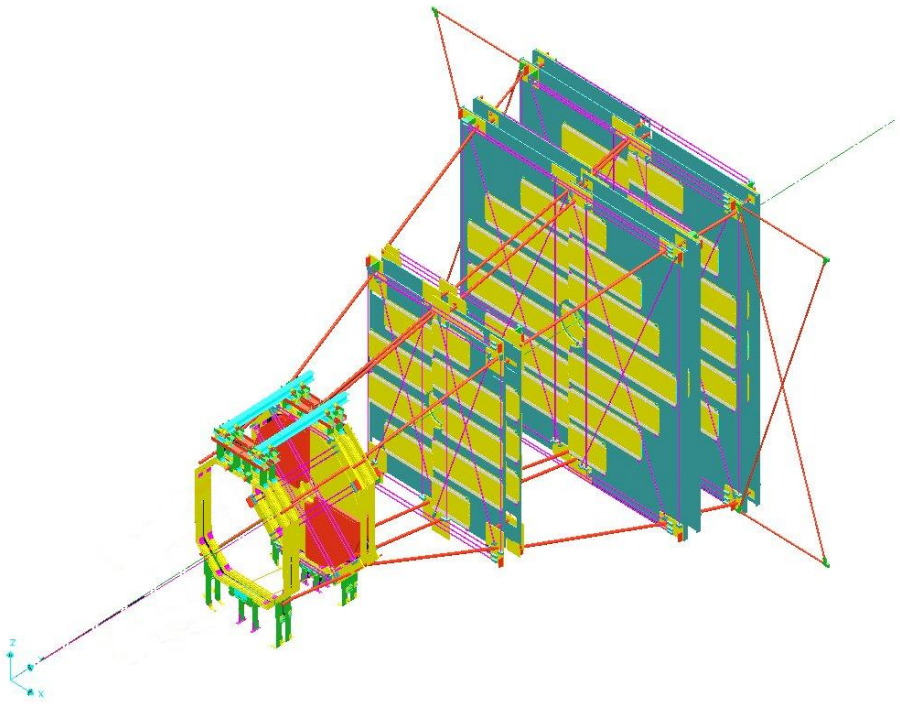

Figure 2: General view of the GMS setup. The red solid lines on this figure represent the optical lines (but are not physical links) between the tracking chambers.

Figure 2 shows a schematic view of the system. The red solid lines represent the optical lines. The GMS is composed of three parts. The first one is the Longitudinal Monitoring System (LMS). Its role is to monitor the relative displacements between the chamber planes. It is composed of BCAM lines linking two neighboring stations and Proximity lines linking the two chambers of each station. The second part is called the Transverse Monitoring System (TMS). It monitors the flatness of the chamber supports. It is only composed of BCAM optical lines. And finally, the last part of the system is the External Monitoring System (EMS). It is composed of eight BCAM lines linking chamber 9 to the cavern walls in order to monitor the absolute displacements of the entire spectrometer.

A simulation of the GMS was developed in order to define the number, the type and the position of the optical devices and to evaluate the performance of the system for the determination of the chamber displacement. In this simulation, various effects as installation accuracy, intrinsic accuracy of the optical devices or thermal gradient effects were included. A complete description of this simulation can be found in [4].

2 Description of the test bench

In order to test the GMS geometry reconstruction program, a test bench of the GMS was built. This bench is a full-scale, aluminium-made mock-up of the three half-planes of chambers 6,7 and 8 of the muon tracking system. It was designed, realized and installed at the LPSC of Grenoble. A picture of the bench is shown in figure 3.

Figure 3: Picture of the test bench.

As the first goal of this bench was to test that the reconstruction program was able

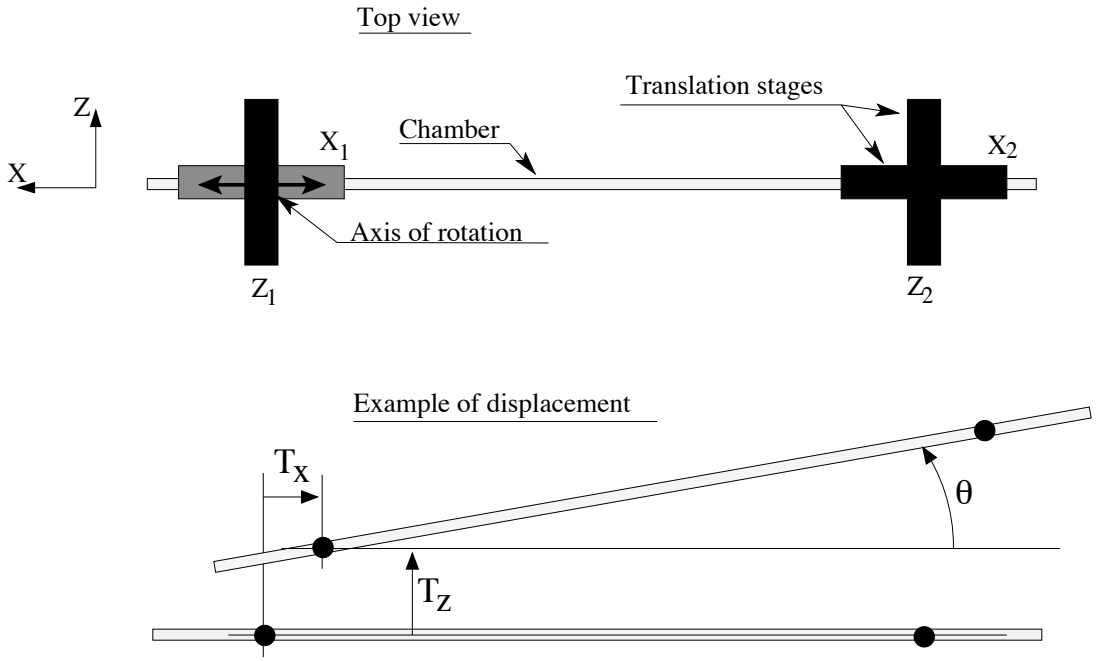

Figure 4: Scheme of the translation system.

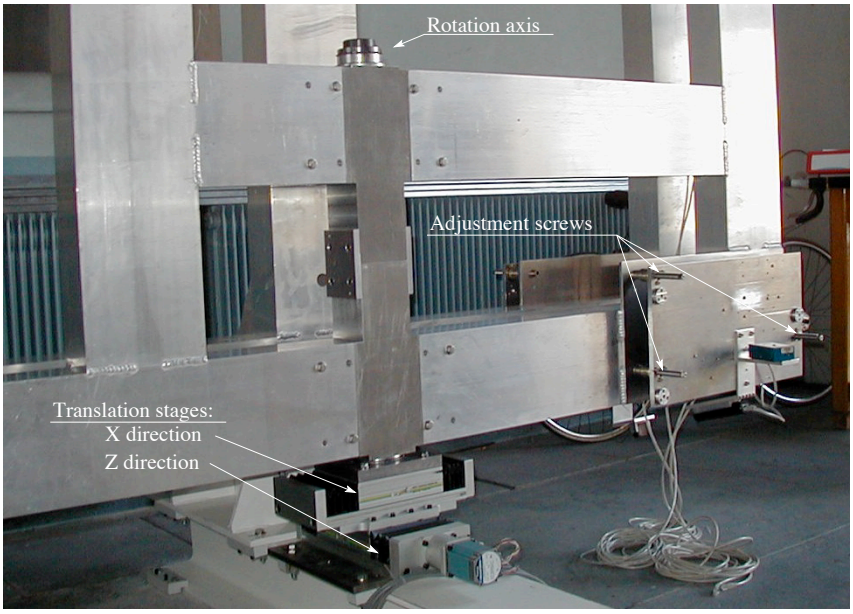

Figure 5: Picture showing the system of translation and the axis of rotation of chamber 7.

to retrieve displacements, we decided to make one of the chambers mobile (chamber 7, see figure 3). Therefore, this chamber was installed on four translation stages, two in the Z direction and two in the X direction, allowing us to have translations in these two directions. The chamber was fixed to the stages using two vertical axes. It is therefore also possible to rotate it around the vertical direction Y. Figure 4 shows a schematic drawing of the displacement system (top) and an example of possible displacement (bottom). Figure 5 shows a detail picture of chamber 7 fixations. The motors used on the stages are stepping motors. Each step corresponds to a displacement of 5 μm. Studies of the accuracy and

the repeatability of these motors were done using a comparator with a precision of 1 μm. This study showed that the standard deviation of the difference between the actual and the requested displacement of the stage controlled with the stepping motor is of the order of 10 μm [5].
The three chambers were equipped with the same number of optical devices as it will be in the ALICE final design, i.e.:

- one BCAM line at each corner for the link between chambers 6 and 7,
- one Proximity line at each corner for the link between chambers 7 and 8,
- six BCAM lines in the plane of each chamber for the monitoring of the deformations of the structure.

3 Survey of the structure

As it is shown in references [3] and [4], an error in the installation of the optical devices induces a loss of resolution in the reconstruction program. The requested accuracy on the optical device position is at the millimeter level.
In order to characterize the test bench geometry, a survey of the complete structure was carried out by the CERN survey group [6]. Each platform supporting the optical devices is equipped with three reference points (named L, M and H, as shown in figure 6). The survey was done in two steps. First, the positions of all reference points were measured and compared to the theoretical positions in 3D space. The left plot of figure 7 shows the differences in the Z direction between the theoretical 3D positions and the measured ones. Their dispersions are of the order of 4 mm with some maximum values of the order of 1 cm. Each platform position in the Z direction was then corrected using the three adjustment screws equipping the platforms (see figure 6). Then, the reference point positions were measured again. The right plot of figure 7 shows the new difference distribution after that adjustment. The dispersion was reduced to about 0.6 mm with a maximum deviation within 2 mm.

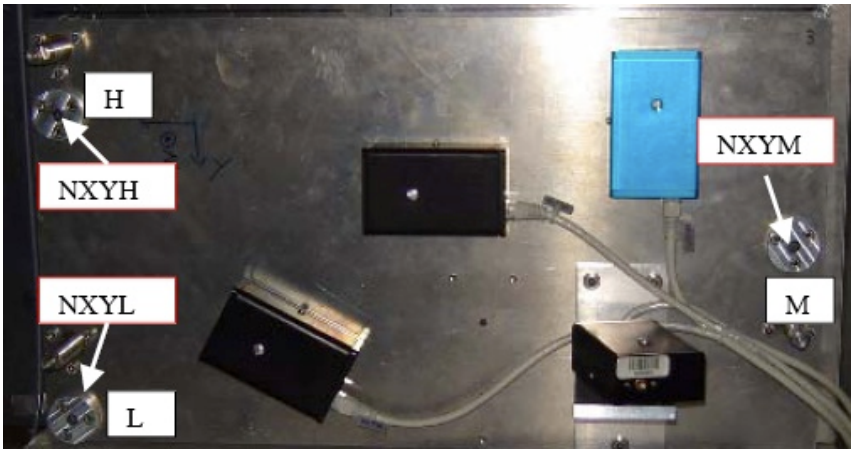

Figure 6: Picture of a platform showing the three reference points.

Table 1 gives the final results from the survey with respect to the 3D theoretical positions and orientations. We can see that chamber 6 is too high by 8 mm and chamber 7 is rotated

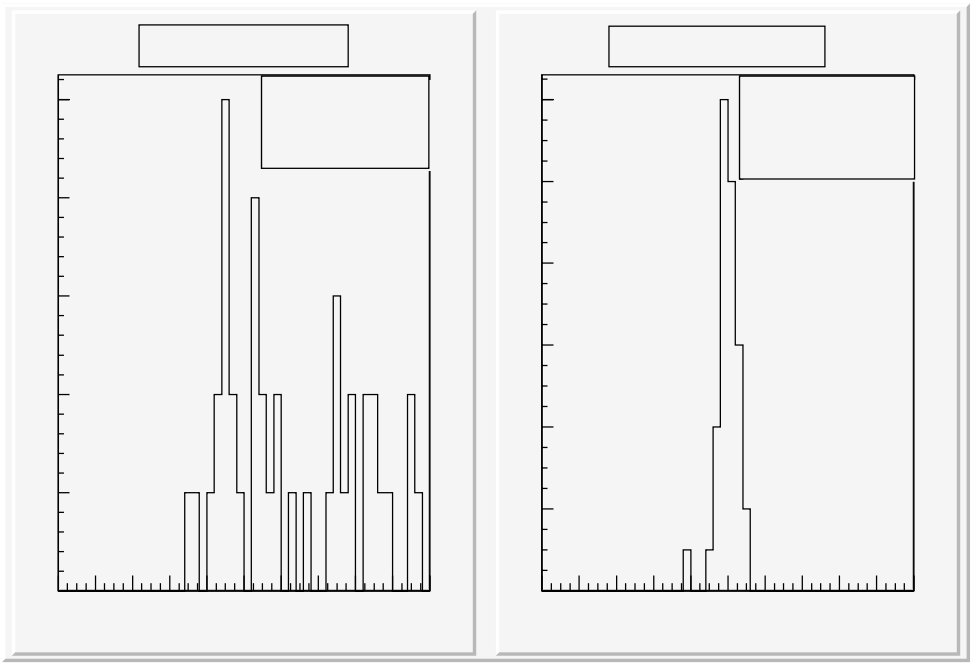

Figure 7: Difference along the Z direction between the theoretical reference point positions and the measured ones before (left) and after adjustment (right).

Chamber	dX (m)	Y + dY (m)	Z + dZ (m)	$d\theta_X$ (rad)	$d\theta_Y$ (rad)	$d\theta_Z$ (rad)
6	$3.6\ 10^{-3}$	$0.79 + 8.4\ 10^{-3}$	$0.00 + 2.2\ 10^{-5}$	$2.0\ 10^{-5}$	$1.5\ 10^{-5}$	$-3.9\ 10^{-5}$
7	$2.2\ 10^{-3}$	$1.28 + 2.8\ 10^{-3}$	$2.59 - 6.2\ 10^{-5}$	$-1.5\ 10^{-5}$	$-7.9\ 10^{-5}$	$-2.0\ 10^{-3}$
8	$6.8\ 10^{-6}$	$1.28 + 1.8\ 10^{-4}$	$3.07 - 1.1\ 10^{-4}$	$-8.2\ 10^{-5}$	$5.1\ 10^{-5}$	$-7.1\ 10^{-4}$

Table 1: Offsets of the measured positions (dX, dY and dZ) and orientations ($d\theta_X$, $d\theta_Y$ and $d\theta_Z$) of the chambers with respect to the theoretical ones (nominal values of X, θ_X, θ_Y and θ_Z are equal to zero, therefore they are not written here).

around the Z direction by 2 mrad ($\sim$0.1 degree). This misalignment of the chambers is small enough so that each object stays within the acceptance of the optical devices. Therefore no change on the structure was done. The chamber positions were entered in the reconstruction program to improve the reconstruction accuracy.

4 Intrinsic resolution of the optical devices

In order to optimize the resolution of the reconstruction program, it is necessary to know the intrinsic resolution of each optical device at the time the measurement were done. This is mainly the resolution in the LED spot finding centroid on the CCD, which includes the thermal fluctuation effects. This quantity is used as weight for each measurement during the χ^2 minimization. This resolution is measured over a long time period run. Images of each optical device are taken many times without any displacement of the chambers. Figure 8 shows the resolution for a typical BCAM. It is of the order of 0.1 μm on the CCD. It corresponds to an angular resolution of about 1.5 μrad (the latter has to be multiplied

by the distance between the source and the CCD to obtain the position resolution of the LED source. The distance between chambers 7 and 8 is about 2 m therefore the resolution on the position of the source LED is about 3 μm). The Proximity resolution is better and is typically of the order of 1 μm for the position of the coded mask.

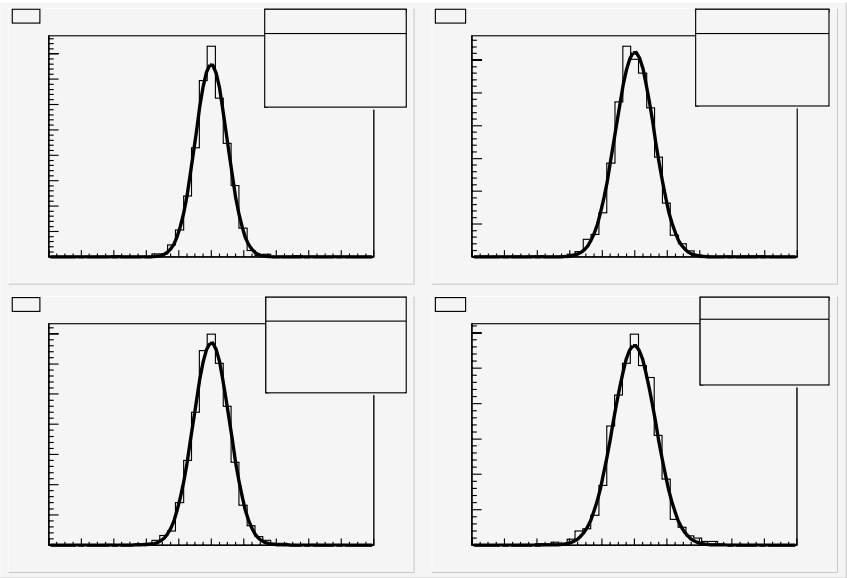

Figure 8: Intrinsic resolution of a typical BCAM for the four different measurements. The units of the horizontal scale are micro-meters.

5 Tests of the reconstruction program

The reconstruction program was developed with simulation purposes in order to define the GMS setup, in terms of optical device number, types and positions, and to estimate its resolution. A detail report on this study can be found in reference [4]. Figure 9 shows a scheme of the reconstruction program procedure. The goal is to retrieve the displacements of the chambers between the initial time T_0 and the current time T_i. T_0 corresponds to the time of the calibration run, where straight muon tracks are collected in order to determine the initial position of the tracking chambers. Using the sets of images obtained at T_0 and T_i, we can determine for each image the displacement of the spot positions on the CCD ($\Delta\ Image_{Mes}$). The reconstruction program is searching, using a χ^2 minimization procedure, to determine chamber displacements (Δ Chamber) that are able to reproduce the same displacements of the images.
In order to check the performance of the reconstruction program to retrieve displacements, we used the translation tables to induced known displacements. Figure 10 shows the results of a test where chamber 7 was translated in the X direction. The left plot shows the displacement measured by the reconstruction program as a function of the induced one. We moved chamber 7 by steps of 100 μm over a range of 2 mm. The measured slope is 0.9999. The right plot shows the residues between the induced displacements and the measured ones. We have here a gaussian shape with a mean compatible with zero and a sigma of about 1.5 μm which is the resolution of the reconstruction convoluted with the

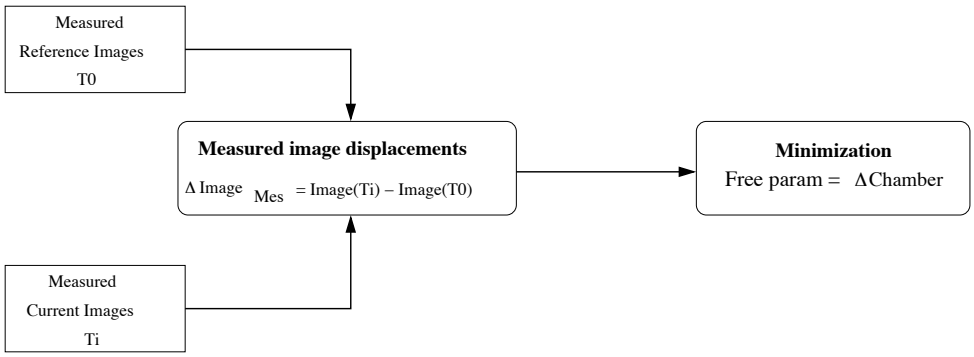

Figure 9: Scheme of the reconstruction program procedure.

resolution on the real displacement measured with the comparators.

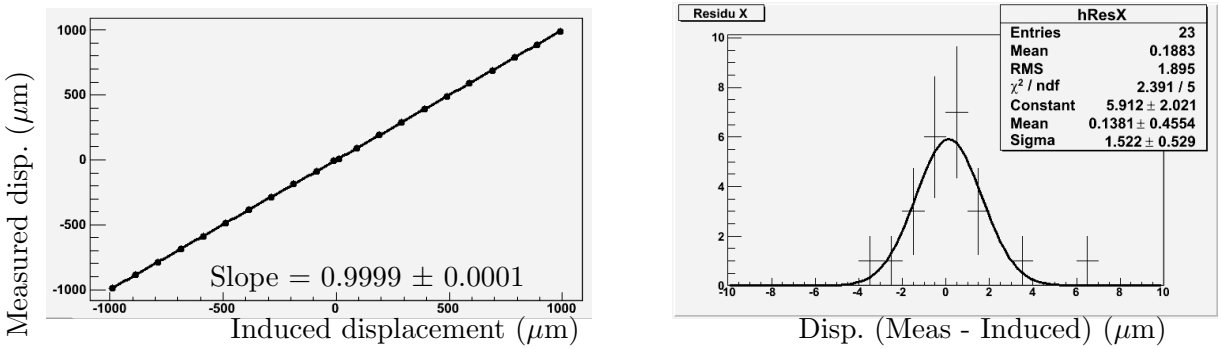

Figure 10: **Left:** displacements measured with the reconstruction program along X versus induced ones for chamber 7, **right:** residues.

Figure 11 shows, with a similar presentation, the result of a test where chamber 7 was translated along the Z direction. We moved it first by steps of 5 μm and then by steps of 50 μm over a range of 250 μm. The sigma of that distribution is about 7.4 μm. The measured slope is 0.986. Contrary to the previous result, a systematic difference of about 1% exists between the measured and induced displacements. This effect has an impact on the mean value of the residues, which is about 2 μm. We were able to retrieve this systematic effect by simulating a systematic shift in the position and orientation of the optical devices. Actually, we discovered that the plates of the platform are not perfectly flat. This induces a mispositioning of the optical elements. In order to minimize this problem, we asked the manufacturer for a better flatness quality for the plates of the final ALICE setup.

As expected, the GMS resolution in the Z direction is worse than in the transverse direction one. This was already shown by the simulation and comes from the fact that the intrinsic resolution of the optical device is better in the direction transverse to the optical axis than in the optical axis direction. We had then reduced this effect by tilting at different angles the four optical lines linking two chambers in order to mix the two directions.

The last test was made by rotating chamber 7 around the vertical axis. Plots of figure 12 show the results of this measurement as a function of the induced angle. The measured

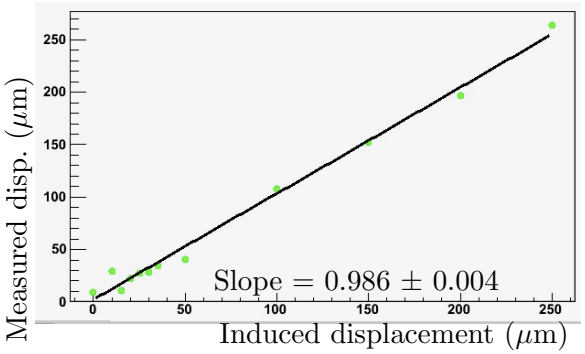

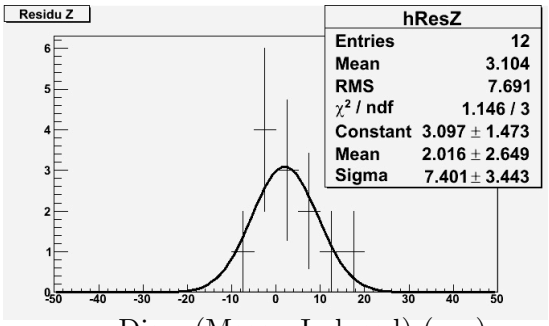

Figure 11: **Left:** measured displacements along Z versus induced ones for chamber 7, **right:** residues.

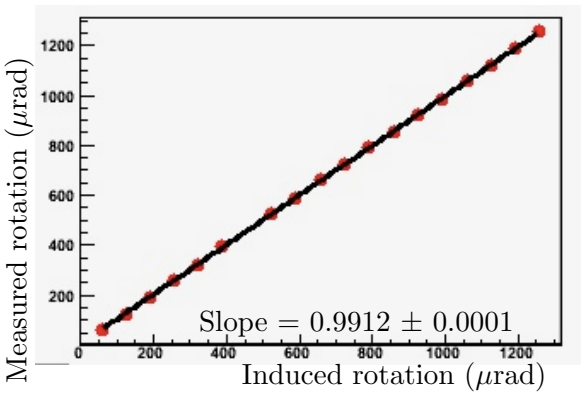

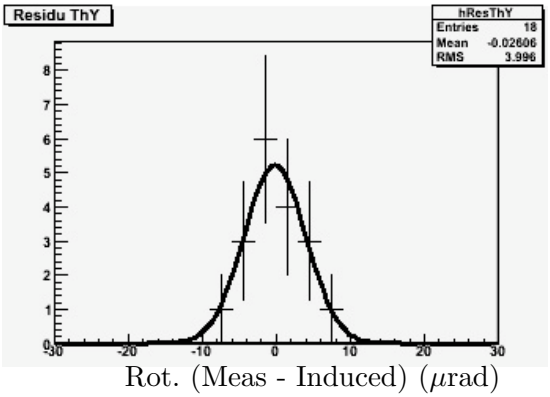

Figure 12: **Left:** measured rotations around Y axis versus induced ones for Chamber 7, **right:** residues.

slope is 0.9912 with an error of 0.0001. It is clear, as in the previous measurement, that we have a systematic error of 1% between the induced and the retrieved rotations. Again, we were able to reproduce this effect by introducing in the simulation a systematic mispositioning of the optical devices. In order to improve the results of this test bench we will need to survey the platforms themselves in order to know the position of the optical devices more precisely. As seen in the right panel of figure 12, the rotation angle is reconstructed with a resolution of 4 μrad.

Figure 13 shows the results of a three days long run without any induced displacement of the chambers. The three plots from top to bottom represent, versus the time, the reconstructed translation and rotation of chamber 7 and the temperature of the room during this period. We can see that a correlation exists between the room temperature and the chamber translation (and/or) rotation. The temperature variations induced a small deformation of the two steel rails ($\lambda_{steel} = 1.2\ 10^{-5}\ ^{\circ}C^{-1}$) on which the three chambers are fixed, and also a deformation of the aluminum chamber structure ($\lambda_{alu} = 2.4\ 10^{-5}\ ^{\circ}C^{-1}$). The deviations are of the order of few tens of μm (or μrad) over the three day period. Into the ALICE cavern, where the temperature variation is of the order of 1 degree, we can expect the same order of magnitude of movement in a stable running condition. From the plots on figure 13 we can extract the reconstruction resolution for the different quantities. In particular, the resolution for the translation along the Y direction (T_Y) and for the rotation around the Z axis (θ_Z) (the two most important parameters for

the muon spectrometer geometry because they have a direct impact on the invariant mass resolution) are respectively 1.1 μm and 0.3 μrad for chamber 7. The resolution for chamber 6 is worst ($\sigma T_Y \simeq 7\mu m$) due to the fact that its position is monitored only by BCAMs which have a worst intrinsic resolution than Proximity. These resolutions are the best we can expect as the running condition in which there were calculated are optimal (no temperature gradient in the room, calm air condition, no vibration).

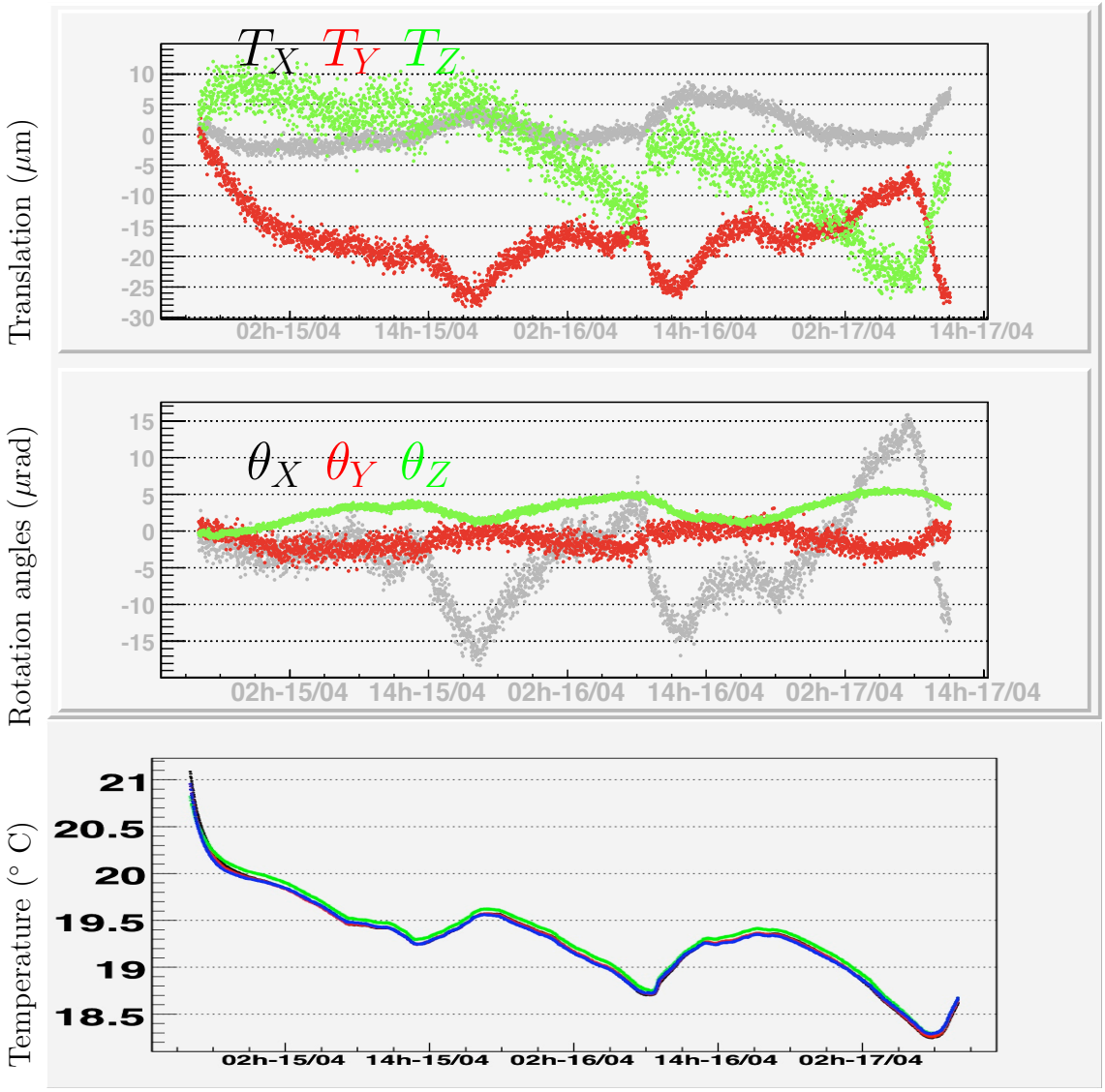

Figure 13: Reconstructed translations (top) and rotations (middle) of chamber 7 versus time, and temperature (bottom) during the same period. T_Y and θ_Z are the most important parameters for the spectrometer as they have a direct impact on the invariant mass resolution.

6 Effects of thermal gradients

Chamber 6 was equipped with a heating pad in order to mimic the power being dissipated by the front end electronics of the tracking chambers. The pad has three separated zones (figure 14). Each zone is equipped with a potentiometer, in order to adjust the power separately. The power dissipated by each zone was tuned according to the temperature map of the station 3 in natural convection which was obtained by simulation [7].

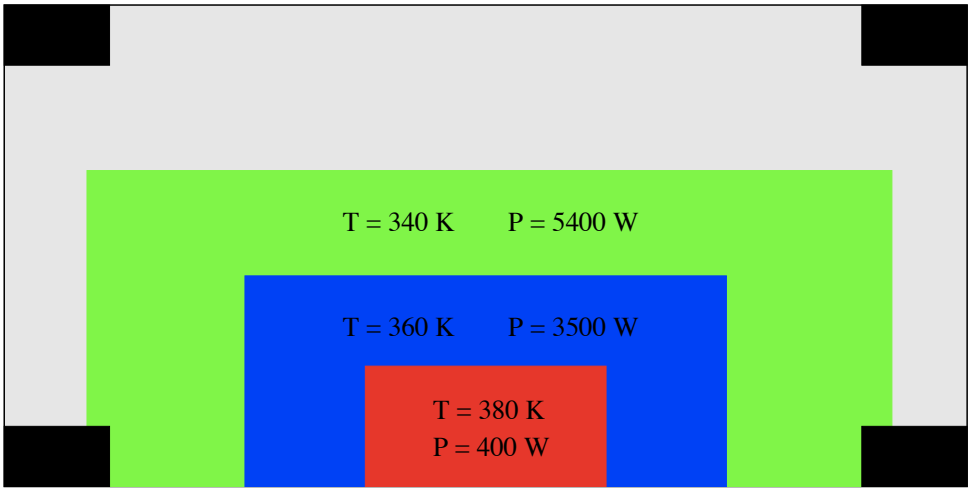

Figure 14: Scheme of the heating pad with its three separated zones of heating. The temperature indicated are the ones at contact.

Figures 15 and 16 show the reconstruction resolutions in the Y position for chambers 6 and 7 respectively. The left plots show this resolution without the heater and the right ones with the heater turned on at its nominal value on chamber 6. We can see that the effect of the thermal gradient is to deteriorate the reconstruction resolution by a factor 4 for chamber 6. On the contrary, it has no effect on the position of chamber 7. In the reconstruction program, chamber 8 is supposed to be fixed. Therefore, the resolution on the position of chamber 7 is driven by the Proximity resolution which links chambers 7 and 8. This explains why the reconstruction resolution for chamber 7 is not affected by the thermal gradients.
The resolution obtained on chamber 6 is about 23 μm. As it has been shown in the reference [3], the resolution should be improved with the utilization of cooling fans. In stations 1, 2 and 3, cool air will be injected at the bottom for stations 1 and 2, and at the bottom and top for the station 3. Thermal study of this cooling has been done for station 3 [7]. We can expect that the resolution obtained here (23 μm) can be reduced. Further tests will be done using two fans blowing air at room temperature.

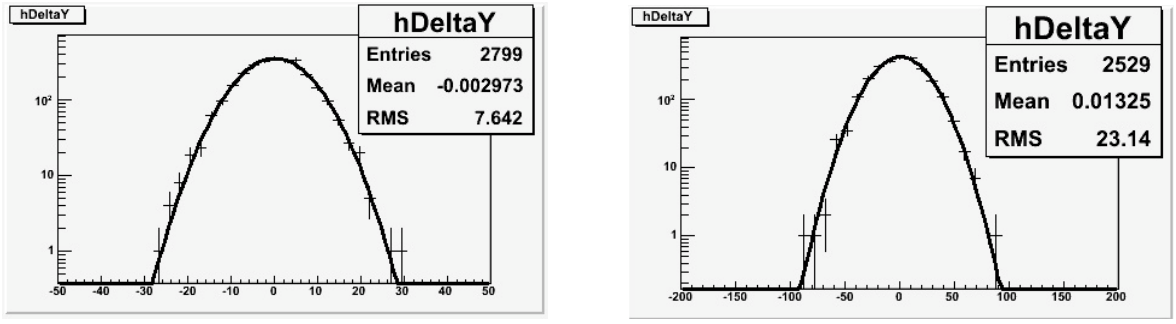

Figure 15: Reconstruction's resolution (in μm) of the Y position of chamber 6, **left:** without any heating, **right:** with the heater turned on at its nominal power (Note the change in scale).

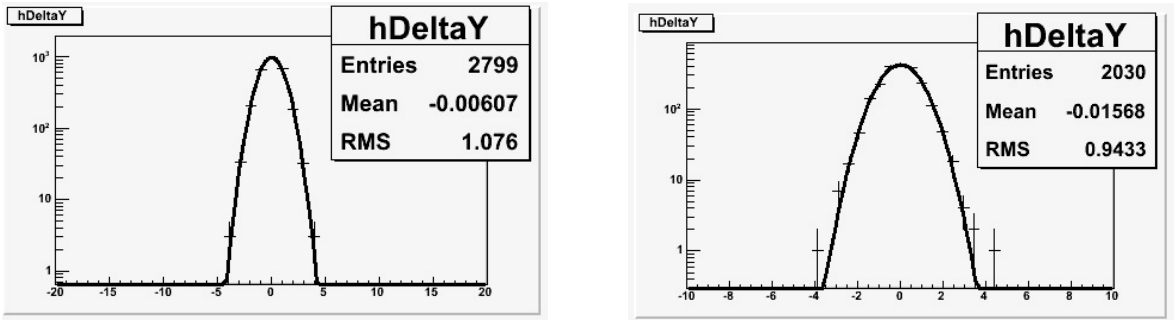

Figure 16: Reconstruction's resolution (in μm) of the Y position of chamber 7, **left:** without any heating, **right:** with the heater turned on at its nominal power(Note the change in scale).

7 Conclusion

In this note, the first results given by the Geometry Monitoring System test bench are presented. The primary goal of this mock up was to test the reconstruction program. It shows that the reconstruction program is able to retrieve with an accuracy of 1.5 μm (in the transverse direction) the displacement induced by the translation stages relatively to chamber 8. Tests with thermal gradient on chamber 6 were done. They show that the resolution on that chamber, relatively to chamber 7, deteriorates from 7 μm (without any thermal gradient) to 23 μm when thermal gradients are generated using an heating pad. This resolution is still better than the requirements which are of the order of 40 μm [4]. Further tests will be done using the two fans that are supposed to reduce those gradient effects.

Acknowledgements

We would like to thank G. Damieux-Verdeau, J.-C. Malacour and S. Roudier from the LPSC workshop, and A. Benoit, G. Gelin and F. Mounier from the IPNL workshop for the construction of the test bench. Also, we would like to thank J.-C. Ianigro for its work in the design of the mechanical supports of the optical devices, and D. Mergelkuhl and V. Prasad from the CERN survey group for their work. We kindly thank P. Stassi and A. Castera from instrumentation groups of the LPSC and IPNL respectively for their help in the definition of the project. The work of V. Kakoyan was partially supported by Calouste

Gulbenkian Foundation from Lisbon, Swiss Fonds Kidagan and the IN2P3-CNRS PICS program 3290.

References

[1] ALICE dimuon forward spectrometer : Technical Design Report, ALICE-TDR-5.- CERN-LHCC-99-022.

[2] ALICE dimuon forward spectrometer : addendum to the TDR, ALICE-TDR-5-add-1.- CERN-LHCC-2000-046.

[3] R. Tieulent et al., ALICE internal note, ALICE-INT-2005-009.

[4] P. Pillot et al., ALICE internal note, ALICE-INT-2005-020.

[5] M. Meziane, Summer student's report (2005).
http://lpsc.in2p3.fr/ALICE/Echange/rapport_stage.pdf

[6] D. Mergelkuhl and V. Prasad, CERN TS/SU survey report, EDMS-702604.

[7] S. Salasca, Progress on cooling of stations 3, 4 and 5, International workshop on dimuon physics in ion-ion collisions at LHC (2003).
http://muonarm.ca.infn.it/afilias/register/dimu03/tuesday/Salasca.ppt